Amino acid containing amphiphilic hydrogelators with antibacterial and antiparasitic activities

ARTICLE

Amino acid containing amphiphilic hydrogelators with antibacterial and antiparasitic activity

Received 00th January 20xx,
Accepted 00th January 20xx

DOI: 10.1039/x0xx00000x

Biplab Mondal,[a†] Vivek Kumar Gupta,[b†] Biswanath Hansda,[a] Arpita Bhoumik,[c] Tanushree Mondal,[a] Hemanta K. Majumder,[c] Charlotte J. C. Edwards-Gayle,[d,e] Ian W. Hamley,[d] Parasuraman Jaisankar*[b] and Arindam Banerjee*[a]

Here we present a series of peptide amphiphiles which form hydrogels based on *beta*-sheet nanofibril networks, several of which have very promising anti-microbial and anti-parasitic activities, in particular against multiple strains of Leishmania including drug-resistant ones. Aromatic amino acid based amphiphilic supramolecular gelators C_{14}-Phe-CONH-$(CH_2)_n$-NH_2 (n=6 for **P1** and n=2 for **P3**) and C_{14}-Trp-CONH-$(CH_2)_n$-NH_2 (n=6 for **P2** and n=2 for **P4**) have been synthesized, characterized, and their self-assembly and gelation behaviour has been investigated in the presence of ultrapure water (**P1**, **P2**, **P4)** or 2% DMSO(v/v) in ultrapure water (**P3**). The rheological, morphological and structural properties of the gels have been comprehensively examined. The amphiphilic gelators (**P1** and **P3**) were found to be active against both Gram-positive bacteria *B. subtilis* and Gram-negative bacteria *E. coli* and *P. aeruginosa*. Interestingly, amphiphiles **P1** and **P3** containing L-phenyl alanine residue show both antibacterial and antiparasitic activity. Herein, we report that synthetic amphiphiles with an amino acid residue exhibit a potent anti-protozoan activity and are cytotoxic towards a wide array of protozoal parasites, which includes Indian varieties of *Leishmania donovani* and also kill resistant parasitic strains including BHU575, MIL^R and CAM^R cells. These gelators are highly cytotoxic to promastigotes of *Leishmania* and trigger apoptotic-like events inside the parasite. The mechanism of killing the parasite is shown and these gelators are non-cytotoxic to host macrophage cells indicating a potential use of these gels as therapeutic agents against multiple forms of leishmaniasis in the near future.

Introduction

In recent years, low molecular weight gelators have been increasingly researchered due to their interesting properties like self-association in a medium to form a linter-linked network structure for various applications.[1-7] These gelators can be assembled using various non-covalent interactions including hydrogen bonding, π-π stacking, van der Waals and other interactions to form gels under suitable conditions.[8] The micro- and nano-network structure of hydrogels leads to a highly porous structure, so they can easily entrap numerous water molecules in the gel cavities.[9] Natural amino acid-based hydrogels are attracting interest not only for the formation of hydrogels via non-covalent interactions but also for their uses in different fields of research work.[10-14] They have wide variety of applications in tissue engineering,[15] cell culture,[16,17] sustained release of drugs and biomolecules,[18,19] drug delivery,[20] vaccine development,[21] wastewater treatment,[14,22,23] wound healing,[24] antimicrobial,[25-32] and others[22,23,33,34]. Peptides and natural amino acid-based supramolecular hydrogels are desirable candidates to prepare biomaterials due to their biocompatibility and biodegradability.[24]

In recent times, the increasing prevalence of bacterial strains with resistance to conventional antibiotics is emerging as a significant threat to modern society.[27] Therefore new types of antibiotics are required to combat such bacteria. The biocompatibility of the natural amino acid-based hydrogels makes them suitable starting materials to develop new antibiotics or biologically active molecules.[25,27] Polycationic peptides containing lysine or arginine moieties can act as antibacterial agents due to their ability to disrupt bacterial membranes.[35-37] Peptides containing hydrophobic and/or cationic residues can be used as molecular building blocks to create antibacterial hydrogels as such peptides can mimic the structure of natural antibiotics.[38,39] In this context, peptide-

[a.] *School of Biological Sciences, Indian Association for the Cultivation of Science, 2A & 2B Raja S. C. Mullick Road, Jadavpur, Kolkata-700032. E-mail: bcab@iacs.res.in*
[b.] *Laboratory of Catalysis and Chemical Biology, Department of Organic and Medicinal Chemistry, CSIR-Indian Institute of Chemical Biology, 2A & 2B Raja S. C. Mullick Road, Kolkata - 700 032, India. Email: jaisankar@iicb.res.in*
[c.] *Infectious Diseases and Immunology Division, CSIR-Indian Institute of Chemical Biology, 2A & 2B Raja S. C. Mullick Road, Kolkata - 700 032, India.*
[d.] *Department of Chemistry, University of Reading, Reading RG6 6AD, U.K*
[e.] *Currently at Diamond Light Source, Harwell Science and Innovation Campus, Chilton, Didcot, Oxfordshire OX11 0DE, U.K.*
†These two authors contributed equally.
*Corresponding authors

Electronic Supplementary Information (ESI) available: Instrumentation, MGC and T_{gel} data, Rheology data, FTIR data, XRD data, SAXS data, Tentative molecular arrangement, Time growth inhibition study, MTT assay data, ROS generation data, Cytotoxicity data, Representative synthetic procedure, Synthesis, Characterisation and spectra (^{1}H, ^{13}C-NMR and HR-MS), References.

based amphiphiles are attractive materials for developing peptide therapeutics as they can be synthesized easily at an affordable cost.[40]

Leishmaniasis holds the second largest position among all parasitic infections after malaria. Recent reports in 2016 by the World Health Organisation suggest that 200,000-400,000 new cases occur every year by visceral leishmaniasis (VL) in 65 countries. Also, visceral leishmaniasis or kala-azar has been found to be endemic, having a 95% of mortality rate if kept untreated.[41] Among the new cases, 90% of the cases have been found in India, Brazil, Somalia, Sudan, South Sudan, and Ethiopia.[42] Specifically, the spread of VL is highly alarming in India and Brazil. In India, annually 100,000 new cases have been occurring, among which, 90% of the cases are found in Bihar. On the other hand, VL has been observed in 21 states out of 27 in Brazil. Unfortunately, until now, chemotherapy is the only choice to combat this disease. Visceral leishmaniasis is characterized by irregular bouts of fever, weight loss, enlargement of spleen and liver and anaemia. VL is endemic in more than 80 countries.[43] If left untreated it is fatal in more than 95% of cases within 2 years after the onset of the disease. Until today, there is no effective vaccine against any form of human leishmaniasis. The problem is even more difficult because of the cases of HIV co-infection.[44] Solutions to overcome these problems include improved chemotherapy and the development of novel drugs specific to these resistant as well as pathogenic strains. Some drugs such as amphotericin B[45] and its lipid formulations, pentavalent antimonials[46] pentamidine, miltefosine, paramomycin, sitamaquine[47] have been used to treat patients. However, the toxicity, side effects, and high cost restrict the use of these drugs. A plausible solution to these issues is the use of chemotherapy[48] and concurrently probing for novel targets showing specificity towards the parasites.

There are reports that amino acid containing peptides and amphiphiles exhibit biologically important applicationsin antibacterials,[25-31] cell culture,[16, 17] and drug release[18, 19, 49]. Many of these molecules contain aromatic amino acid residues like L-phenylalanine[27] and L-tryptophan.[12] However, the development of aromatic amino acid containing amphiphilic gelators with antiparasitic activity is unprecedented to the best of our knowledge. The previous reports also suggest that organic heterocyclic compounds such as oxindoles, can be excellent material against parasites *L. donovani*. Thus, we chose L-tryptophan (and for reference L-phenylalanine) as components of our gelator amphiphiles. We have synthesized four amphiphiles containing proteinaceous aromatic amino acids L-phenylalanine and L-tryptophan with varying chain length of the cationic $-NH_2$ containing polar head group, and with a fatty acyl chain of fourteen carbon atoms at the C-terminus. At first, gelator amphiphiles **P1**, **P2**, **P3** and **P4** containing L-phenylalanine or L-tryptophan (Fig. 1a) were synthesised and studied for antiparasitic and antibacterial activity. However, it was observed that only **P1** and **P3** are active towards parasite *L. donovani* and also against Gram-positive and -negative bacteria. Thus, L-phenylalanine has a role in antiparasitic and antibacterial activity. Our results also show that methylene units (CH_2) attached to the terminal amino groups do not have any role in either antiparasitic or antibacterial property. From the comprehensive experimental data, it was evident that both molecules **P2** and **P4** containing L-tryptophan are unable to kill both protozoan parasite *Leishmania donovani* or Gram positive and Gram negative bacteria.

Experimental section

Materials and methods

Chemicals

L-Phenylalanine (Phe), myristic acid (C_{14}), HOBt (1-hydroxybenzotriazole), DCC (N, N'-dicyclohexylcarbodiimide), di-tert-butyldicarbonate (BOC Anhydride, DiBOC), silica gel (100−200 mesh), and aluminium oxide (basic) were purchased from SRL, India. N, N'-dimethylformamide (DMF), trifluoroacetic acid (TFA), hexamethylenediamine, sodium dihydrogen phosphate, and disodium hydrogen phosphate were purchased from Merck. Millipore Mili-Q grade water was used for all experiments. Dimethyl sulfoxide (DMSO), camptothecin and penicillin-streptomycin solution were purchased from Sigma Chemicals (St. Louis, MO, USA). 3-(4, 5-Dimethyl-2-thiazolyl)-2, 5-diphenyl-2H-tetrazolium bromide (MTT) was purchased from Invitrogen Life Technologies (Carlsbad, CA, USA). All drugs were dissolved in 100% DMSO at a concentration of 25 mM and stored at -20°C. MitoSOX red (M36008), MitoTracker green (M7514), TMRM (T668), CM-H2DCFDA (C6827), FITC Annexin V/Dead Cell Apoptosis kit (V13242) were obtained from Molecular Probes.

Synthesis and Characterisation

The amino acid containing gelator amphiphiles were synthesized by conventional solution phase coupling methods using a racemization-free fragment condensation strategy. The characterisation of the synthesis products was done using mass spectrometry, ^{1}H NMR spectroscopy and ^{13}C NMR spectroscopy. All NMR studies were carried out using a Bruker DPX 400 MHz or Bruker DPX 500 MHz spectrometer at 300 K. Concentrations were in the range 5−10 mM in $CDCl_3$ or DMSO-d_6. Mass spectra were recorded on a Q-Tof micro (Waters Corporation) mass spectrometer by positive mode electrospray ionization process.

Preparation of gels

15 mg of **P1**, 10 mg of **P2**, and 10 mg of **P4** gelator amphiphiles have been weighed into three different sets of 5 mL screw-capped glass vials with the addition of 1 mL of ultrapure water (Mili-Q) in each one. Then the glass vials were heated on a hot plate till the gelator molecules were dissolved completely. After that, the heated glass vials were cooled in a water bath for 5 min. Later these solutions were kept at room temperature 28 ^{o}C for a few minutes to a few hours, depending on the gelator molecules, to form stable gels.

For gelator amphiphile **P3**, 10 mg of amphiphile has been added to 980 µL of mili-Q water and heated on a hot plate until the solute gelator amphiphile was dissolved. Then 20 µL of DMSO was added to the heated solution before cooling it in a water bath as well as room temperature (at 28 ^{o}C). The formation of stable co-solvent-induced gelation was observed within one hour.

Loading of Hydrogel onto Rheometer

Firstly, hydrogels were removed from the 5 mL glass vial using a scoopula. These hydrogels were further loaded onto the Peltier plate without any air or bubbles into the hydrogels. Then these hydrogels were placed at the centre of the Peltier plate. After that, a program was used to set the height of the cone to the 27 µm height gap. When the gap height is reached, trim the edges of the hydrogel with a pipet tip so that the hydrogel correctly fills the geometry. Then the solvent trap was placed over the geometry and onto the Peltier plate and it surrounded the outer edges of the solvent trap with water to keep the hydrogel hydrated during the data acquisition.

General procedure for antibacterial study

A well-established agar well cut-diffusion method was employed to analyze the antibacterial activity of amphiphilic gelators against four pathogenic strains of Gram-positive (*S. aureus* and *B. subtilis*) and Gram-negative (*E. coli* and *P. aeruginosa*) bacteria. A measurable quantity of HiMedia agar (HA) was liquefied in ultra-pure deionized water and stirred vigorously to obtain a homogenous mixture. The homogeneous solution was autoclaved for about 30 min, after which 20 mL of the autoclaved mixture was trickled in each of the sterilized Petri plates and allowed to form gel for 30 min. The gel plates were placed in an incubator for 12 h at 37 °C to identify the presence of any adventitious bacteria. After that, four known bacteria were spread on the fresh agar gel medium one by one. The gel well was cut to introduce the gel samples. The gel samples of **P1** to **P4** were placed at that position to identify the antibacterial properties of the gelator amphiphiles. The sample-charged plates were gently positioned for incubation at 37 °C temperature for 24 h to enhance the complete diffusion of the gelator amphiphiles. The inhibition zones of each plate were measured and recorded in millimeter (mm) units.

Parasite maintenance and culture

Four strains of Leishmania donovani were used: (i) the sodium antimony gluconate (SAG)-sensitive (SAGS) MHOM/IN/1983/AG83, (ii) multidrug resistant field isolate MHOM/IN/2009/BHU575/0 (BHU 575),[50] (iii) laboratory grown miltefosine-resistant (MILR) strains, (iv) camptothecin resistant (CPTR) strain, also (v) Leishmania major was used in the study. Amastigotes obtained from the spleens of infected hamsters were cultured at 22 ^{o}C to obtain promastigotes.[51] The promastigotes were cultured in M199 medium containing 20 % (v/v) heat-inactivated fetal bovine serum (FBS-Gibco Life Technologies, Carlsbad, California, USA) supplemented with 100 IU/mL of penicillin and 100 mg/mL of streptomycin solution at 22 ^{o}C. Promastigotes were further grown in 10% (v/v) heat-inactivated FBS for 5-6 days at 22 ^{o}C before use. To observe the ultrastructure alterations of the parasites, 1×10^{6} cells were treated with different concentrations of amphiphilic gelators for 8 and 12 h and observed under microscope. DMSO was used as a vehicle control.

Leishmania promastigotes cell viability measurement

The *L. donovani* AG83 wild type strain, multidrug resistant (BHU 575), laboratory grown MIL^{R} cells, CPT^{R} cells and *L. major* strain were individually incubated with different concentrations of amphiphilic gelators for 24 h, following which the viability was assessedusing a MTT assay.[52] Yellow MTT (3-(4, 5-dimethyl-2-thiazolyl)-2, 5-diphenyl-2H-tetrazolium bromide) is reduced to purple formazan in the mitochondria of the living cells. The formazan is then solubilised, by adding isopropanol and 6(N) HCl and the concentration determined by taking OD at 595 nm. Living cells actively convert MTT to formazan, thereby generating a quantitative measure of viability and cytotoxicity. All IC_{50} and IC_{90} values were calculated using a variable slope model to find EC50 using prism (version 5.0, GraphPad software, San Diego, CA; USA). We further investigated the effect of drugs on survivability of *Leishmania* promastigotes using light microscope by direct microscopic counting in a haemocytometer. The cells of the exponential phase of the growth curve were used in the study. Briefly, cells were collected and transferred onto a 24-well tissue culture plate (2 × 10^{6} cells/well). Cells were then left to incubate at various concentrations of amphiphilic gelators (1.0, 2.5, 5.0, 10.0 and 20.0 µM) for 12 h at 22 ^{o}C. After incubation the cells were collected and centrifuged and the pellet was washed with 1x PBS twice and finally resuspended in 1x PBS. Aliquots 50 µL were mixed with 0.4% solution of trypan blue and incubated for 3 min at 22 ^{o}C. About 5-7 µL of mixture was carefully transferred to haemocytometer and the blue (dead) and clear (live) cells were counted. The total number of viable cells in mixture was measured by multiplying the total number of viable cells by 2 (the dilution factor for trypan blue). Percentages of viable cells were calculated using the formula:

$$\text{Percentage viability} = \left(\frac{\text{Live cell count}}{\text{Total cell count}}\right) \times 100$$

Measurement of ROS

The level of intracellular reactive oxygen species (ROS) were measured using cell-permeable, non-polar probe H2DCFDA (molecular probes, Eugene, USA). For measurement of ROS in treated and untreated parasites, 2 × 10^{6} cells were treated with amphiphilic gelators (0.5, 1.0, 2.5 and 5.0 µM) for 12 h. Promastigotes treated with 0.2% DMSO served as controls. After incubation, parasites were washed with phosphate buffer saline and resuspended in 500 µL of PBS (without phenol red) and stained with the cell-permeant dye H2DCFDA for 15-20 min.[53] In another set of reaction the parasites were incubated with N-acetyl cysteine (NAC) prior to treatment with amphiphilic gelators. The green fluorescence of 2′, 7′-dichlorofluorescene (DCF) was measured at 530 nm using a flow cytometer. All the fluorometric measurements were performed in triplicate, and the results were expressed as the mean fluorescence intensity per 10^{6} cells.

Measurement of mitochondrial membrane potential (Ψm)

Mitochondrial membrane potential was investigated using tetramethylrhodamine, methyl ester (TMRM). Healthy mitochondrion membranes maintain an electrical potential between the interior and exterior of the organelle, referred to as a membrane potential. TMRM is a cell-permeant dye that accumulates in active mitochondria with intact membrane potentials. If the cells are healthy and have functional

mitochondria, the signal is bright. Upon the loss of mitochondrial membrane potential, TMRM accumulation ceases and the signal disappears. In brief, after different treatments with amphiphilic gelators (0.5, 1.0, 2.5 and 5.0 µM), *Leishmania* cells were harvested and washed with 1x PBS. Cells were then incubated at 37 ^{o}C for 30 min with a final concentration of TMRM dye at 0.2 µM.[54] In another sets of reactions the parasites were treated with 1.0 µM respiratory uncoupler carbonyl cyanide m-chlorophenylhydrazone (CCCP) added as positive control 1 h before treatment with amphiphilic gelators **P1** and **P3**. To check the effect of ROS quenching, cells were pre-treated with 10 mM N-acetyl cysteine (NAC) an anti-oxidant for 2 h before amphiphilic gelator treatment, and FACs analysis were performed. TMRM signal can be detected with flow cytometry using 488 nm laser for excitation and 570 ± 10 nm emission filters. The spectrofluorometric data presented here are representative of three independent experiments.

Determination of mitochondrial Superoxide levels

After oxidative phosphorylation, mitochondrial superoxide is generated as a by-product. Approximately 2-4% of mitochondrial oxygen consumed is incompletely reduced in a tightly coupled electron transport chain and leads to ROS production.[55-57] The levels of mitochondrial superoxide were measured by MitoSOX Red, which is a mitochondrial superoxide indicator (M36008, Invitrogen). MitoSOX is a fluorogenic dye, specific for mitochondrial superoxide, which is cleaved after interacting with $O2^{-}$ produced by the mitochondria, and after binding with DNA emits red fluorescence. The experiment was performed according to manufacturer's protocol. Briefly, 1 × 10^6 cells were treated with different concentrations of amphiphilic gelators **P1** and **P3** and incubated for 12 h at 22 ^{o}C. After incubation cells were washed with 1x PBS at 300 g for 1 min. The supernatant was discarded and 100 µL of 1x PBS was added to the sample. Cells were stained with MitoSOX Red at 200 nM concentration for 30 min at 37 ^{o}C in the dark and were analyzed by flow cytometry (BD FACS).

Double staining with annexinV and PI

Apoptotic events i.e. progression of cell through different stages of cell death is measured by staining with annexinV and propidium iodide (PI). Cells were treated with amphiphilic gelators (0.5, 1.0, 2.5 and 5.0 µM) and apoptosis was measured by using an annexinV dead cell apoptosis kit (Invitrogen Life Technologies, Carlsbad, California, USA). Experiments were carried out for untreated and treated promastigotes. The FL-1 and FL-2 channels denote the mean intensity of FITC-annexinV and mean intensity of PI so appropriate gating was done. The experiments were performed three times and an average of three experimental spectrofluorometric data were expressed as mean ± SD.

Isolation of gDNA

To check the size of DNA fragments formed during cell death, total genomic DNA were isolated according to manufacturer's protocol (QIAGEN genomic DNA isolation kit) and analyzed by agarose gel electrophoresis. Briefly, 1 × 10^7 cells/mL of *L. donovani* promastigotes was treated with amphiphilic gelators (2.5 and 5.0 µM) for 12 h respectively. Then, the pellets were washed with 500 µL PBS buffer. The pellets were re-suspended in 200 µL PBS. Twenty µL proteinase K and 4 µL RNase A were added and kept for 30 min at 37 ^{o}C. Then, 200 µL buffer AL were added to the solution and mixed by vortexing for 15-20 sec. The above solution was heated for 10-15 min at 56 ^{o}C and ultracentrifugation was performed at 3000 rpm for 10-15 s to remove the drops from the lid. Then 200 µL of 100% ethanol were added and mixed by vortexing for 10-15 sec. The above samples were carefully applied to the column and centrifuged at 6000 g for 1 min. Then 500 µL of buffer AW1 were added to the column and the samples were centrifuged at 6000 g for another 1 min. QIAamp mini-columns were placed into another 2 mL collection tube and 500 µL of buffer AW2 was added, mixed and centrifuged at 20000g for 3 min. The column was again placed on a new 2 mL centrifuge tube and the above samples were re-centrifuged for another 1 min to complete the removal of the wash buffer. Final elution was done by adding 200 µL AE buffer. The total cellular genomic DNA from all the samples was subjected for fragmentation analysis by 1% agarose gel electrophoresis analysis.

DNA fragmentation assay

Genomic DNAs were isolated with an apoptotic DNA ladder kit (Roche Applied Science, Penzberg, Upper Bavaria, Germany) from exponentially growing AG83 strain of *Leishmania donovani* promastigotes (2 × 10^7 cells/mL) with or without any prior treatments with amphiphilic gelators for 4 h. DNA were electrophoresed in 1.5% agarose gel at 75 V, stained with ethidium bromide and photographed under UV illumination.[59] An estimate of the extent of DNA fragmentation after drug treatments was detected using cell death detection ELISA kit (Roche Diagnostics). Promastigote samples (5 ×10^6 cells/mL) were collected after 0, 4, 6 and 8 h. Post-treatments with these amphiphilic gelators and the cytoplasmic-histone-associated DNA fragments (mononucleosome and oligonucleosome) were detected using the manufacturer's protocol. DNA fragmentation was detected by spectrophotometric measurement of microtiter plates in a thermo MULTISCAN Ex plate reader at 405 nm. Relative percentage was plotted as units of time.

Atomic force microscopy

The AFM studies were performed to observe any morphological changes in the *Leishmania donovani* promastigotes after treatment with the amphiphilic gelators **P1** and **P3**. An Agilent Technologies 5500 ILM Pico plus AFM system with a piezo scanner maximum range of 100 µm was used for this experiment. All the images were obtained in contact mode by using micro-fabricated silicon cantilevers of 450 µm length with a nominal spring force constant of 0.02–0.77 N/m from Nano sensors (Neuchatel, Switzerland). The cantilever oscillation frequency was tuned to resonance frequency, 6–21 kHz. The *Leishmania donovani* promastigotes (1 × 10^6 cells/mL) were incubated with medium M199 containing 1.25 µM of amphiphilic gelators (IC_{50} value of both the amphiphilic gelators) for 12 h. Then the cells were again washed (1100 g for 15 min at room temperature) and fixed in 4% (w/v) paraformaldehyde. The fixed cells were then diluted

1:10 with milli Q water. Aliquots 10 µL of diluted sample were then deposited on a freshly cleaved muscovite Ruby mica sheet (ASTM V1 Grade Ruby Mica from MICAFAB, Chennai, India) and kept for 5–10 min for air drying. Mica sheets are negatively charged so samples bind strongly to the mica surface. After drying, the samples were gently washed with 0.5 mL milli-Q water and again kept for drying. The images of the samples were captured at a scan rate of 0.5 lines/sec. Images were processed by using Pico view 1.12 version software (Agilent Technologies, Santa Clara, CA, USA). Image manipulation was done through Pico Image Advanced version software (Agilent Technologies).

Culture of Leishmania donovani axenic amastigotes

Promastigotes of *Leishmania donovani* were used for cultivation of axenic amastigotes. By varying medium constituents, pH, temperature and culture time axenic amastigotes were obtained. Conversion of promastigotes into amastigotes was achieved by growing promastigotes in 3 mL of low pH (5.5) axenic amastigotes media supplemented with 10% fetal bovine serum at 37 ^{o}C for 7-10 days. Axenic amastigotes were grown in ventilated flasks at 37 ^{o}C with 5% CO_2 supply. After growth, all parasites had a round morphology without emerging flagella.

Measurement of dose-dependent cytotoxic effect of these amphiphilic gelators on cultured murine peritoneal macrophages by MTT assay

Macrophages isolated from mice were seeded on a 96-well tissue culture plate (approximately 10^5 cells/mL**)** in RPMI complete media supplemented with 10% FBS and left to adhere for 48 h at 37 ^{o}C under 5% CO_2 supply. Macrophages were then treated with increasing concentrations of these amphiphilic gelators (10, 20, 50, and 100 µM) for 72 h. Percentage of viable promastigotes was measured by MTT assay by measuring OD at 570 nm in a spectrophotometer reader.

Statistical analysis

Data are provided as mean value ± SEM or mean value ± SD, of the number of independent experiments. Data were tested for significance by using the paired student t-test. Differences were considered statistically significant when p values were <0.05. Statistical analysis and graphical representation was performed with GraphPad prism.

Results and discussions

Gelation study

The amphiphilic gelators consist of a natural aromatic amino acid residue such as L-phenylalanine or L-tryptophan, long fatty acyl hydrophobic chain, and a terminally placed polar head, containing $–NH_2$ as a functional group. In this regard, four amphiphiles, **P1**, **P2**, **P3**, and **P4**, (Fig. 1a) were synthesized by introducing two different amino acids L-phenylalanine or L-tryptophan with the variation of polar $–NH_2$ head containing a diamine derivative. The Fig. 1a shows the chemical structures of these gelator molecules. The aromatic

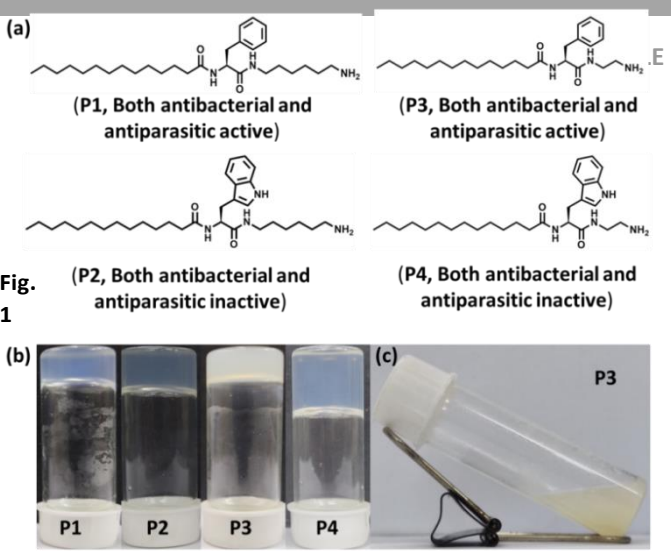

Fig. 1 (a) Chemical structures and the activity of amphiphilic gelators **P1**, **P2**, **P3** and **P4** used in antibacterial and antiprotozoal study, (b) hydrogels obtained from amphiphilic gelators (**P1**, **P2** and **P4**) in ultrapure water and in 2% DMSO (v/v) mixed in ultrapure water for **P3** respectively, (c) viscous solution of **P3** in only ultrapure water.

amino acid, L-phenylalanine, or L-tryptophan was selected to promote the π-π stacking interaction between the gelator molecules. The hydrophobic fatty acyl chains were introduced to promote van der Waals and hydrophobic interactions, and the terminally located polar amine ($–NH_2$) group as a head group was used to increase the polarity of the gelator amphiphile. Moreover, the gelator molecules were designed in a way so that they can quickly form a stable hydrogel in the presence of a polar aqueous solvent. It was found that the gelators P1, P2, and P4 form stable hydrogels in the presence of ultrapure water (mili-Q)(pH 6.67) at a concentration of 0.65-1.20% w/v of gelator molecule (Fig. 1). The gelator molecule P3 does not form a hydrogel in ultrapure water alone, but it exhibits a viscous aggregated solution. However, **P3** forms a hydrogel in 2% v/v of DMSO mixed in water (Fig. 1b,c). During the experimental analysis, the viscous solution of gelator P3 has been used for further experiments to keep the environment same for all these gelator amphiphiles.

Thermal Stability of Gels

Gel-to-sol transition temperatures (T_{gel}) of these hydrogels (**P1**, **P2**, and **P4)** were measured to determine the thermal stability of these hydrogels. The gel transition temperature (T_{gel}) was highest for **P2** and lowest for **P1**, keeping the gelator concentration 31.68 mM fixed. As mentioned above, the amphiphile **P3** does not form hydrogel in ultrapure water but forms a viscous solution. However **P1** with a longer terminal diamine unit did forma hydrogel. The L-tryptophan-based amphiphilic gelators **P2** and **P4** show higher thermal stability than **P1**. The gel-to-sol transition temperature shows the following trends: **P2**>**P4**>**P1** (Table S1). It is evident that the gelator **P2** with the highest van der Waals interaction and strong π-π interaction shows the best-ordered packing structure compared to **P1** and **P4**. The gelator **P4** forms a more robust hydrogel than that of **P1**. This may be due to the fact that L-tryptophan residue shows better π-π interactions than that of the L-phenylalanine containing amphiphiles (**P1** and **P3**)

as L-tryptophan has a greater π-electron containing surface area than L-phenylalanine.

Rheological study

The rheological experiments were carried out at the gelators' constant concentration of 31.68 mM. The frequency sweep experiment was performed at a fixed strain of 0.1% for all the amphiphile gelators. The two moduli, storage modulus (G') and loss modulus (G''), have been plotted against angular frequency (ω) ranging from 0.05 to 100 rad/s. The storage modulus (G') is always greater than that of loss modulus (G''), indicating a stable gel formation. Rheological studies have been performed for gelators **P1**, **P2** and **P4** at a fixed concentration of 31.68 mM for all cases (**P3** does not form a hydrogel). As discussed above, the stability order of gels is **P2**>**P4**>**P1** corroborated with T_{gel} values**,** which is also reflected in the moduli measured in the frequency sweep experiments. The storage moduli of **P1**, **P2**, and **P4** are 0.28 × 10^2 Pa, 2.34 ×10^4 Pa and 1.31 × 10^4 Pa respectively at a constant strain of 0.1% and at a fixed concentration 31.68 mM of the individual gelator (Fig. S1). The amplitude sweep experiments also show the gels' linear viscoelastic region (LVE) limits. The hydrogels formed by the gelator amphiphiles **P1**, **P2**, and **P4** show a tolerance limit between 0.01% to 0.72%, 0.01% to 0.98%, and 0.01% to 2.18% of shear strain (Fig. S2) respectively. Cross-over between G' and G'' took place when 20%, 3.48 %, and 7.85% of the shear strain were applied to the **P1**, **P2**, and **P4** hydrogels, respectively. Thus the mechanical stability follows the thermal stability of these hydrogels in the order **P2**>**P4**>**P1**.

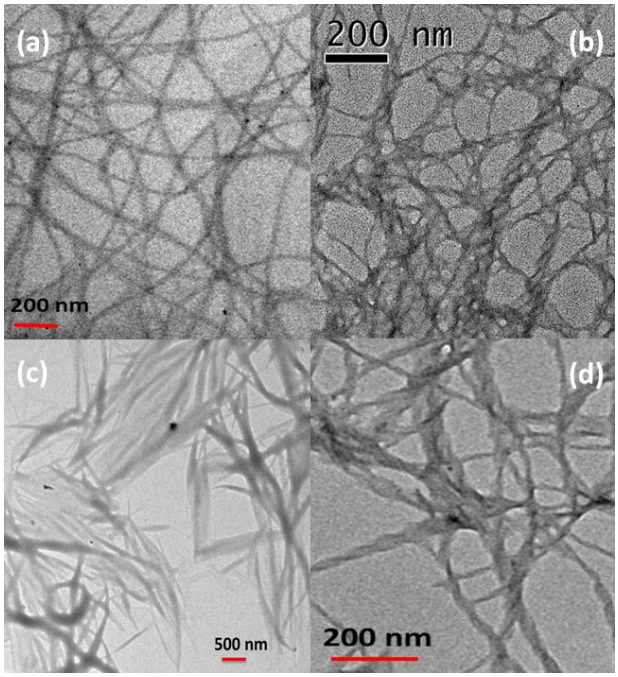

Fig. 2 HR-TEM images of dried (a) hydrogel of amphiphile **P1**, (b) hydrogel of amphiphile **P2**, (c) viscous solution of amphiphile **P3**, and (d) hydrogel of amphiphile **P4** in presence of ultrapure water.

Morphological study

High-resolution transmission electron microscopic (HR-TEM) imaging was used to probe the morphological features of these hydrogels (Fig. 2). The L-phenylalanine-containing gelator amphiphile **P1** forms a nano-fibrous network structure in the gel, whereas **P3** forms sheet-like morphology in the viscous solution. The morphologies differ due to the distinct states of the solutions. The L-tryptophan-containing amphiphilic gelators **P2** and **P4** form hydrogels and the morphology comprises twisted nano-fibres (Fig. 2). HR-TEM images show the cross-linked nano-fibrous network structure in the hydrogels. The fibres are several nanometres in length, and the width varies from 17.10 nm to 30.67 nm, with an average width of 23.24 nm. However, the majority of these nano-fibres have a width between 20 nm to 25 nm (Fig. 2). Even the Cryo-TEM (Cryogenic transmission electron microscopic) images have been taken for the amphiphiles **P2** hydrogel and **P3** viscous solution, to know whether any change in morphology take places in HR-TEM in dry state or not. However, the Cryo-TEM images show that the **P2** forms nano-fibres net-work structure and **P3** forms sheet like morphology by a bunch of fibres (Fig. S3) like their respective HR-TEM images (Fig. 2b,c).

FTIR study

Fourier transform infrared (FT-IR) spectroscopy was used to understand non-covalent interactions among the gelator molecules in the gel state during self-assembly. The FTIR spectra of dried gels and the aggregated solution for amphiphilic gelators contain four signature peaks at 3466 cm^{-1}, 3298 cm^{-1}, 1648 cm^{-1}, and 1556 cm^{-1} (Fig. S3).The peaks at 3298 cm^{-1} and 1556 cm^{-1} correspond to the hydrogen bonding N–H stretching and bending frequencies, respectively. The strong signal at around 1648 cm^{-1} is due to the amide C=O stretching frequency of the aggregated gelator molecules. Lastly, the peak at 3466 cm^{-1} is due to the non-hydrogen bonded N–H stretching frequency of the gelator molecules. The broad peak at 3466 cm^{-1} with the highest intensity indicates the presence of mainly free N–H in the aggregated state of **P3**. Moreover, the minimum intensity of the 3466 cm^{-1} peak for **P2** indicates that most N–H units are involved in the H-bond formation in the gel state. This data are consistent with the thermal stability measurement data, as the hydrogel formed by the **P2** gelator was the strongest one. The FTIR data revealed a hydrogen-bonded are consistent with a sheet-like structure during the self-assembly of gelator molecules in the gel state (Fig. S4).

XRD analysis

Wide-angle X-ray diffraction (XRD) study was performed for dried gels (**P1**, **P2**, **P4**) and dried sol (**P3**), respectively, to understand the non-covalent interactions between the amphiphilic gelator molecules. This study also helps us to understand the inter-sheet and inter-planer distance between the amphiphilic gelators. The d-spacing values between 3.69-3.78 Å peaks are due to the π-π stacking interactions between aromatic residues present in the respective amphiphiles in their gel and viscous solution states.[23] The peaks corresponding to 2θ in the range 18.20°–17.62° (d=4.74–4.90 Å) are due to the formation of a β-sheet-like structure by the

amphiphilic gelators in their aggregated states (Fig. S5).[27] A peak with a d-spacing of 9.12–9.20 Å (2θ = 9.43–9.35°) suggests the formation of a β-sheet-like alignment of these gelators in their respective gel state. The d-spacing values in the range 4.74–4.90 Å corresponds to the distance between the peptide chains formed by the gelator molecules within a β-sheet-like backbone structure, while the peaks in the range 9.12-9.20 Å can be attributed to the distance between two β-sheet layers formed in the gel state (Fig. 3).[25]

SAXS study

Small-angle X-ray scattering (SAXS) has been used to get more insight into the supramolecular network structure formed by the gelator molecules in their gel state. The similar SAXS patterns were observed for **P1**, **P2** and **P4** amphiphilic gelator in their gel state (Fig. S5) indicate the formation of a similar type of morphology in their gel states. The *d*-spacing values of **P1**, **P2** and **P4** amphiphilic gelators in their gel state are 35.81 Å, 40.28 Å and 34.95 Å respectively (Fig. S6).

The amphiphilic gelator **P2** shows a *d*-spacing value of 40.28 Å (Fig. S7), which is higher than the molecular length 26.75 Å but smaller than twice this value, 53.50 Å (Fig. S6), indicating that the molecules are interdigitated. Thus, a tentative molecular model has been constructed based on the FTIR, XRD, and SAXS data (Fig. 3).

Antibacterial Study

Most of the reported natural peptide antibiotics generally contain N-terminal L-lysine and/or L-arginine.[29] Reports also demonstrate antibacterial activity of cyclicpeptides.[35, 36] Li and co-workers report that the L-tryptophan-based self-assembling peptide shows strong interaction with the lipidic membrane of bacteria, which led to the death of *E. coli* and *S. aureus* bacteria.[12] Also, L-tryptophan is present in various classes of antimicrobial peptides.[58] But in this report, the lack of antibacterial activity of L-tryptophan-based amphiphilic gelators makes this paper more exciting. Interestingly, some of the amphiphilic gelators, **P1** and **P3** were highly active against both Gram-positive and Gram-negative bacteria. Antibacterial activities for the viscous solution of amphiphile **P3** and hydrogels **P1**, **P2**, and **P4** were investigated for different kinds of pathogenic bacteria, such as Gram-positive *B. subtilis* and *S. aureus* for and Gram-negative *E. coli* and *P. aeruginosa* using the agar well diffusion method. As shown in Fig. 4, L-phenylalanine gelators show very high activity against both bacteria. Both of these amphiphiles (**P1** and **P3**) were highly active against Gram-positive bacteria *B. subtilis* and Gram-negative bacteria *E. coli* and *P. aeruginosa*. Both **P2** and **P4** amphiphiles were dormant against all four bacteria used in this experiment (Fig. 4). **P2** and **P4** were inactive even at higher 650 µg/mL concentrations. The inhibition zone formed by the amphiphiles **P1** and **P3** in the screening test proves the antibacterial activity for the **P1** hydrogel and **P3** for viscous solution. The zone of inhibition studies using amphiphiles **P1** and **P3** indicate sufficient inhibition zones for these compounds to be classed as antibiotic. The zone of inhibition diameters for **P1** against *B. subtilis*, *P. aeruginosa*, and *E. coli* were 22 mm, 26 mm, and 20 mm, respectively (Table 1). For **P3**, the zone of inhibition diameters against *B. subtilis*, *P. aeruginosa*, and *E. coli* were 22 mm, 28 mm, and 18 mm, respectively (Table 1). The minimum inhibitory concentration (MIC) values of the gelator amphiphiles (**P1** and **P3**) against Gram-positive bacteria (*B. subtilis*) and Gram-negative bacteria (*P. aeruginosa* and *E. coli*) were determined by using the microdilution technique. Gram-positive bacteria *B. subtilis* show a similar zone of inhibition diameter of 22 mm for both **P1** and **P3** at a fixed concentration of 320 µg/mL, whereas their MIC values are 40-80 µg/mL and 40-120 µg/mL respectively. The MIC value for *E. coli* was 100-200 µg/mL for **P1** and **P3**. Amphiphilic gelators **P1** and **P3** show MIC values of 80-130 µg/mL and 70-140 µg/mL respectively for the bacteria *P. aeruginosa*. Both gelators **P2** and **P4** were inactive against all the bacteria used throughout the antibacterial study, even up to a concentration of 650 µg/mL. Moreover, time growth inhibition study using different bacterial population upon the lead hydrogels were performed to establish the stability of the hydrogelator for a longer duration of time (Fig. S8).

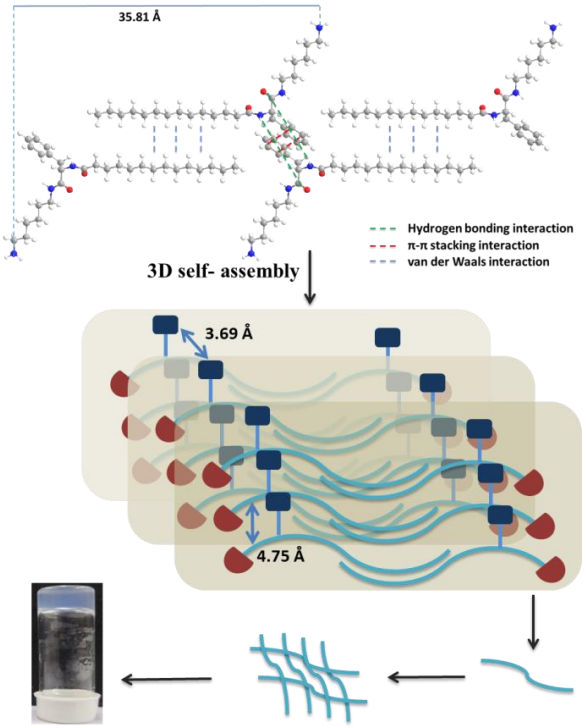

Fig. 3 A tentative model of intermolecular arrangements in the hydrogel obtained from **P1** derived from FTIR, XRD, and SAXS data.

Table 1. List of bacterial zone of inhibition (**ZOI**) diameter in mm by agar-well diffusion method and minimum inhibitory concentration (**MIC**) by **P1** and **P3** amphiphile on Gram-negative and Gram-pasative bacteria.

Bacteria	P1		P3	
	ZOI (mm)	MIC	ZOI (mm)	MIC
P. aeruginosa	26	80-130 µg/mL	28	70-140 µg/mL
B. subtilis	22	40-80 µg/mL	22	40-120 µg/mL
E. coli	20	100-200 µg/mL	18	100-200 µg/mL
S. aureus	–	–	–	–

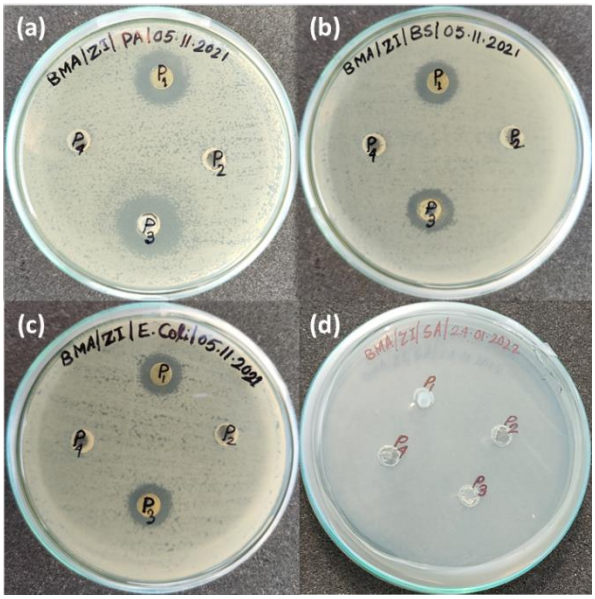

Fig. 4 Effect of hydrogels on Gram-negative and Gram-positive bacteria by agar well diffusion method against: (a) *P. aeruginosa*, (b) *B. subtilis*, (c) *E. coli* and (d) *S. aureus*. The concentrations of the hydrogels were 320 µg/mL in all cases.

Anti-parasitic activity

Both amphiphilic gelators **P1** and **P3** show cytotoxicity against wild type AG83 as well as drug resistant *L. donovani* promastigotes. The Cytotoxic potential of four different amphiphilic gelators on *Leishmania* promastigotes was checked using MTT assays. SAG-sensitive *L. donovani* AG83 parasites (2×10^6 cells/mL) were left for incubation with these four amphiphilic gelators (25 µM for 12 h). Data showed that only **P1** and **P3** have cytotoxicity against *Leishmania* promastigotes (Fig. S9). Treatments of *L. donovani* wild type AG83 strain, *Leishmania major*, multidrug resistant (BHU-575) strain, Miltefosine resistant (MIL^R) strain and Camptothecin resistant (CPT^R) strain (2×10^6 cells/mL) with seven different concentrations of amphiphilic gelators **P1** and **P3** (0.25 µM, 0.5 µM, 1.00 µM, 2.50 µM, 5.00 µM, 7.50 µM and 10.00 µM) for 12 h were evaluated by MTT assay. This study demonstrated a dose-dependent cytotoxic effect towards parasitic growth. Promastigotes treated with amphiphilic gelators **P1** and **P3** showed that at 12 h, 94% and 99% of total number of AG83 promastigotes were killed by 7.5 µM and 10.0 µM concentrations respectively (Fig. 5a). In the case of *Leishmania major* parasite growth study only 1% cells were viable after treatment with 10 µM concentration of amphiphilic gelators (Fig. 5b). On the other hand, for the multidrug resistant (BHU-575) parasite, only 2% and less than 1% of total number of parasites were viable after treatments with 10 µM concentration of amphiphilic gelators **P1** and **P3** (Fig. 5c). Moreover, MIL^R parasites treated with amphiphilic gelators **P1** and **P3** with a concentration of 10 µM showed that only 1.0 to 1.5% viability after 12 h of treatment (Fig. 5d). Similar results were seen with CPT^R parasites, where only less than 1.0% and 1.5% parasites were viable after treatments with amphiphilic gelators **P1** and **P3** respectively (Fig. 5e). Controls containing 0.2% DMSO were incubated separately in the experiment and data showed no adverse effect on the parasite viability. The EC_{50} and EC_{90} values of amphiphilic gelators **P1** and **P3** against all strains (AG83, Ld Major, BHU-575, MIL^R and CPT^R) of *L. donovani* were calculated using variable slope model (Prism, GraphPad Software, Version 5.0, San Diego, CA) and these data are presented in table 2. Miltefosine was used as a positive control. We also measured

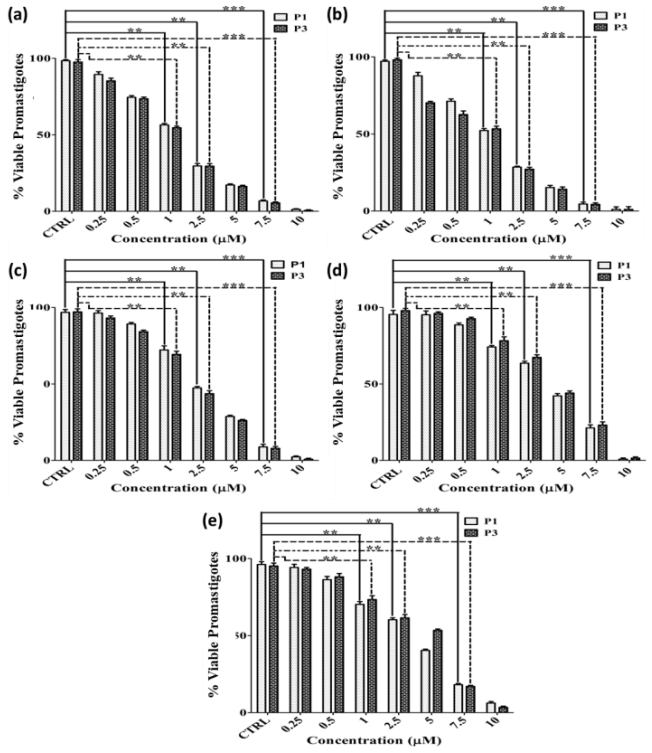

Fig. 5 Cytotoxic effect of aromatic amino acid containing amphiphilic gelators **P1** and **P3** on *Leishmania* promastigotes. Analysis of *in vitro* dose-dependent cytotoxicity of **P1** and **P3** by MTT assay. Log phase (a) AG83 promastigotes cells (b) Ld Major promastigote cells (c) BHU-575 promastigotes cells (d) MIL^R promastigote cells (e) CPT^R promastigote cells were cultured for 12 h in M199 media. Percentages of viable promastigotes were measured by MTT assay. All data expressed as percentage of live promastigotes and represent mean ± S.D. from three independent experiments. *P<0.01, **P<0.001, ***P<0.0001 compared with control, by the Student t-test (a to e).

Table 2. EC_{50} and EC_{90} values for the effect **P1** and **P3** on *Leishmania* promastigotes growth measured by MTT assay.

Drug	Promastigotes	EC_{50} (µM)	EC_{90} (µM)	Miltefosine EC_{50} (µM)
P1	AG83	1.148 ± 0.0012	7.237 ± 0.0016	19.827 ± 0.0009
	Ld Major	1.045 ± 0.0013	7.068 ± 0.0014	15.362 ± 0.0017
	BHU-575	2.376 ± 0.0011	7.402 ± 0.0016	20.235 ± 0.0013
	MIL^R	3.420 ± 0.0011	8.560 ± 0.0014	>100
	CPT^R	4.193 ± 0.0012	8.243 ± 0.0015	19.713 ± 0.0012
P3	AG83	1.153 ± 0.0012	7.145 ± 0.0016	19.827 ± 0.0009
	Ld Major	1.071 ± 0.0013	7.054 ± 0.0014	15.362 ± 0.0017
	BHU-575	2.218 ± 0.0011	7.329 ± 0.0016	20.235 ± 0.0013
	MIL^R	3.832 ± 0.0011	8.776 ± 0.0014	>100
	CPT^R	5.364 ± 0.0012	8.138 ± 0.0015	19.713 ± 0.0012

Table 3. EC_{50} and EC_{90} values for the effect of **P1** and **P3** on *Leishmania* promastigotes growth obtained by trypan blue exclusion method.

Drug	Promastigotes	EC_{50} (μM)	EC_{90} (μM)	Miltefosine EC_{50} (μM)
P1	AG83	0.972 ± 0.0010	6.952 ± 0.0014	19.627 ± 0.0011
	Ld Major	1.037 ± 0.0014	7.281 ± 0.0011	14.971 ± 0.0009
	BHU-575	1.982 ± 0.0013	6.994 ± 0.0013	19.826 ± 0.0010
	MIL^R	2.967 ± 0.0011	7.956 ± 0.0011	>100
	CPT^R	4.233 ± 0.0010	8.817 ± 0.0014	19.544 ± 0.0007
P3	AG83	1.042 ± 0.0011	7.145 ± 0.0014	19.627 ± 0.0011
	Ld Major	0.931 ± 0.0012	7.054 ± 0.0011	14.971 ± 0.0009
	BHU-575	2.121 ± 0.0013	7.329 ± 0.0014	19.826 ± 0.0010
	MIL^R	3.672 ± 0.0013	8.776 ± 0.0011	>100
	CPT^R	4.984 ± 0.0010	8.138 ± 0.0014	19.544 ± 0.0007

the viability of the AG83 promastigotes along with BHU-575 and MIL^R parasites by direct microscopic counting using trypan blue exclusion method and obtained similar results to the MTT assays. The EC_{50} and EC_{90} values obtained using this method are included in table 3.

Oxidative stress and formation of reactive oxygen species (ROS) inside the cell

It has been reported that unlike in other mammalian cells, camptothecin (CPT) induces oxidative stress in *Leishmania donovani* cells.[59] It was reported that, during oxidative phosphorylation, the release of ROS inside the cells in the form of superoxide anions occurs in the extent of 4-6% of total O2 consumed.[60] However, sometimes under certain conditions when drug inhibits oxidative phosphorylation, there is an increase in the production of ROS.[60] To identify the effect of these amphiphilic gelators on intracellular ROS generation, Leishmania promastigotes were separately treated with P1 and P3 at four different concentrations (0.5, 1.0, 2.5 and 5.0 μM) for 12 h (Fig. 6a). In another set of experiments, the time course effect of amphiphilic gelators on ROS generation was measured. Promastigotes were treated with anti-oxidant NAC (10 mM for 2 h) prior to the treatment with both the amphiphilic gelators (5 μM). Intracellular ROS generations were measured fluorometrically by conversion of CM-H2DCFDA to highly fluorescent 2′, 7′ dichlorofluorescein after treatment with these amphiphilic gelators in L. donovani promastigotes. The level of peroxide radicals gradually increased inside the cell with increase in time in a dose dependent manner of P1 and P3. Briefly, the fluorescence intensity was significantly increased at 5.0 μM concentration in comparison to 1.0 and 2.5 μM concentrations (Fig. 6b). When promastigotes were treated with NAC prior to treatment with amphiphilic gelators, the ROS generation decreased. The above experimental data leads to the conclusion that the generation of total cellular ROS at 12 h primarily induces the downstream progress of programmed cell death (PCD).

Even, we have performed a FACs analysis on mammalian fibroblast cell to check the levels of reactive oxygen species (ROS) generated before and after the treatment with the hydrogelator amphiphliles. We treated the cells with amphiphliles **P1** and **P3** (25, 50, 75 and 100 μM) for 48 h and checked the levels of ROS production using flow cytometer (Fig. S10). Result shows that at 100 μM concentration of amphiphliles **P1** and **P3** only 3-4 % ROS are generated, which is considered as a negligible amount.

Depolarization of mitochondrial membrane potential (Ψm)

Depolarization of mitochondrial membrane potential was determined by using TMRM (200 nm for 30 min at 37 °C),[61] which is colourless, positive charged dye that enters in a membrane potential dependent manner inside mitochondria and emits bright red orange fluorescence that was analyzed by flow cytometry (BD FACs). Flow cytometric analysis (Fig. 7a) revealed that promastigotes treated with P1 and P3 showed pronounced depolarization of Ψm. Penetration of TMRM dye

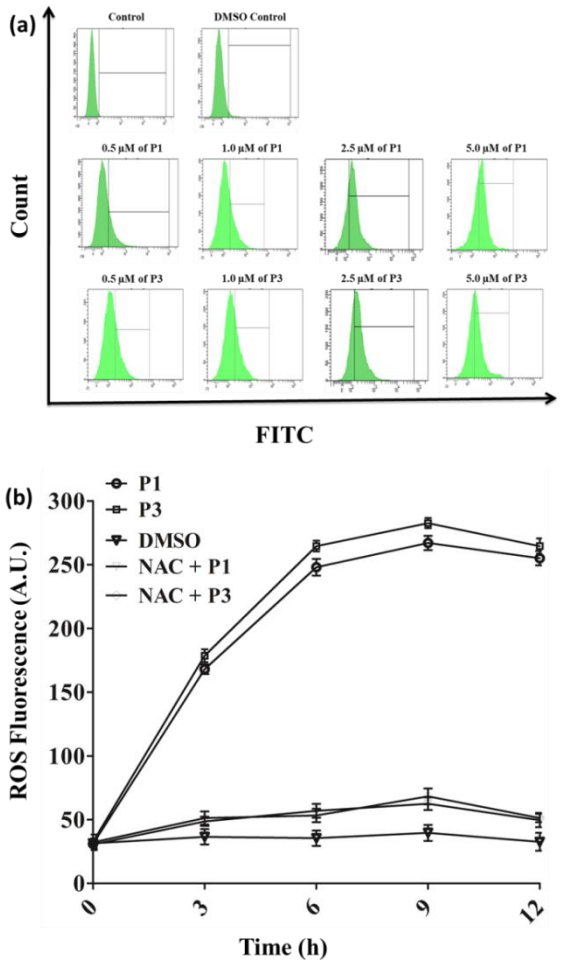

Fig. 6 Flow cytometric analysis of ROS generation inside L. donovani promastigotes induced by **P1** and **P3**. Measurements of induced ROS generation. (a) Generation of peroxide radicals within the L. donovani promastigotes was measured after treatment with 0.2% DMSO, peptide **P1** (0.5, 1.0, 2.5 and 5.0 μM) and **P3** (0.5, 1.0, 2.5 and 5.0 μM) as described in Materials and Methods section. After incubation with H2DCFDA the fluorescence intensity was measured at 530 nm by flow cytometry. (b) Formation of peroxide radicals within the leishmanial promastigotes were measured after treatment with 0.2% DMSO, **P1** (5μM), **P3** (5μM), and NAC (10 mM) treatment prior to the treatment with **P1** and **P3** for 3, 6, 9 and 12 h.

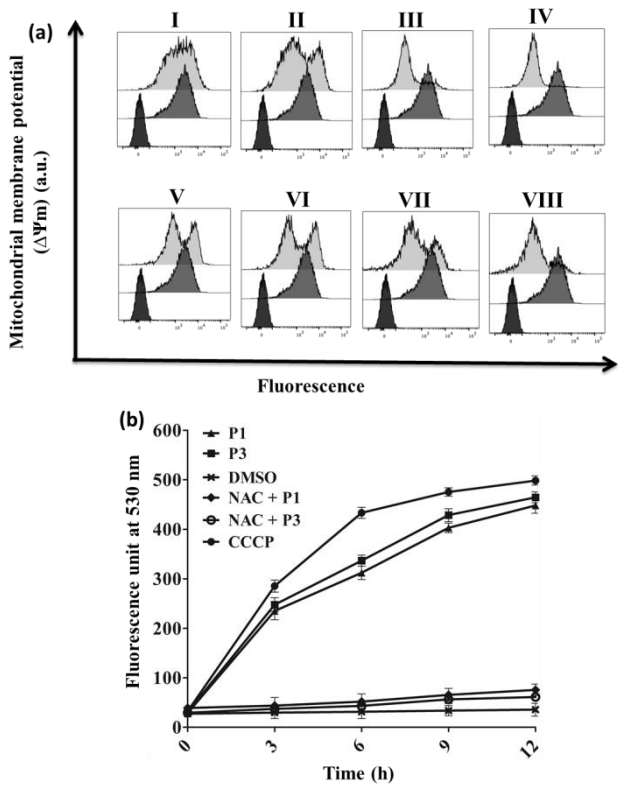

Fig. 7 (a) Fluorescence-activated cell sorting (FACS) analysis of mitochondrial membrane potential (Ψm) using TMRM before or after treatment with gelator amphiphile **P1** 0.5, 1.0, 2.5 and 5.0 µM (panel I to IV) and **P3** 0.5, 1.0, 2.5 and 5.0 µM (panel V to VIII) for 12 h in *Leishmania* cells. TMRM fluorescence was plotted against cell numbers (count). Bottom panel indicates unstained cells (without any stain) whereas middle panel indicates control cells (treated with 0.2% v/v DMSO). (b) Fluorometric analysis of ΔΨm. Changes of ΔΨm after treatment with 0.2% DMSO alone and with Peptide **P1** (5 µM), with uncoupling agent CCCP (5 µM) as positive control and NAC an anti-oxidant (10 mM) as negative control prior to treatment with **P1** (5 µM) and **P3** for 0, 3, 6, 9 and 12 h.

through mitochondrial membranes is an effective discrimination between healthy and apoptotic cells. Depolarization of Ψm is an early event of apoptosis and one of the characteristic features of cellular apoptosis. To investigate the role of these amphiphilic gelators on depolarization of Ψm a time course study was performed (Fig. 7b). The promastigotes of *Leishmania* cells were treated with an uncoupling agent of mitochondria i.e. carbonyl cyanide m-chloro-phenylhydrazone (CCCP, 1.5 µM) as a positive control that causes complete depolarization of Ψm. A significant 82-85% increase in mean green fluorescence intensity was observed after 12 h treatment with **P1** and **P3** (2.5 µM) as compared to relative Ψm measured after treatment with CCCP. The green fluorescence intensity was further increased to an extent of 92-98% upon treatment with 5 µM concentration of amphiphilic gelators for 12 h. When cells were treated with an anti-oxidant such as NAC (10 mM) prior to treatment with amphiphilic gelators progression of Ψm is halted and the mean green fluorescence intensity was measured which were significantly same as DMSO treated cells.

P1 and P3 induce the generation of mitochondrial superoxides anion in *L. donovani* parasites

Our results show that the amphiphilic gelators induce depolarization of mitochondrial membrane potential inside the parasites. We further investigate the generation of superoxide radicals formation inside the mitochondria. The generation of superoxides anions was measured by MitoSOX red staining through flow cytometric analysis. The amphiphilic gelators P1 and P3 increased the levels of superoxide anions in a dose-dependent manner inside the parasites (Fig. 8a). It was found that about 90-95% of parasites were positive for superoxide radicals at 5 µM concentration of both the amphiphilic gelators (Fig. 8b).

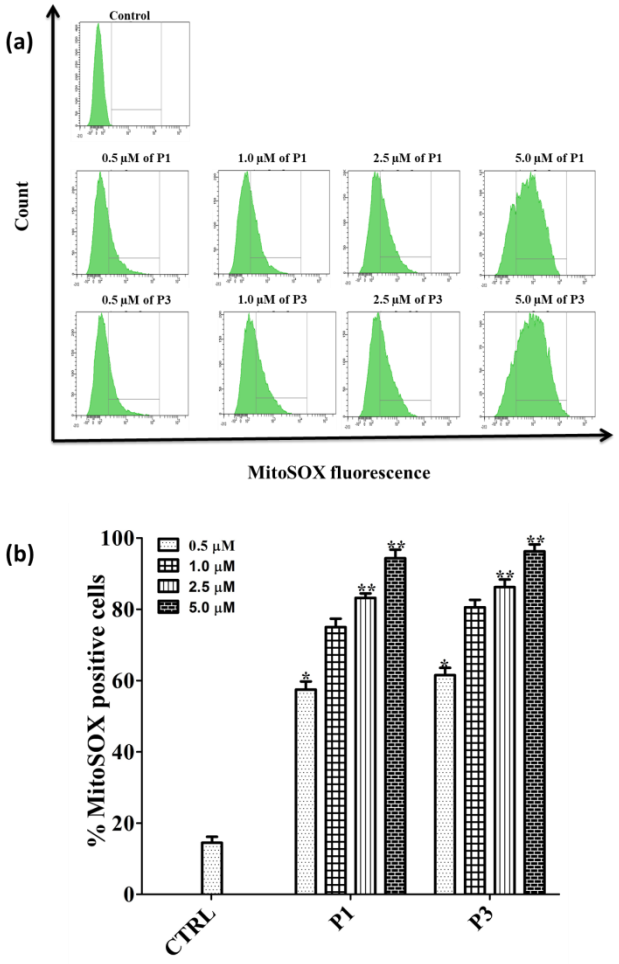

Fig. 8 (a) Flow cytometric analysis of P1 and P3 induced mitochondrial superoxide generation inside *L. donovani* promastigotes using fluorescent dye MitoSOX red. (b) Bar graph representation of mean % of superoxide positive cells. Flow cytometric analysis of histogram showing superoxide positive cells of *L. donovani* promastigotes induced by P1 and P3. Data represent means ± SD (n=3). *P<0.01, **P<0.001 compared with without any pretreatment control, by the Student t-test.

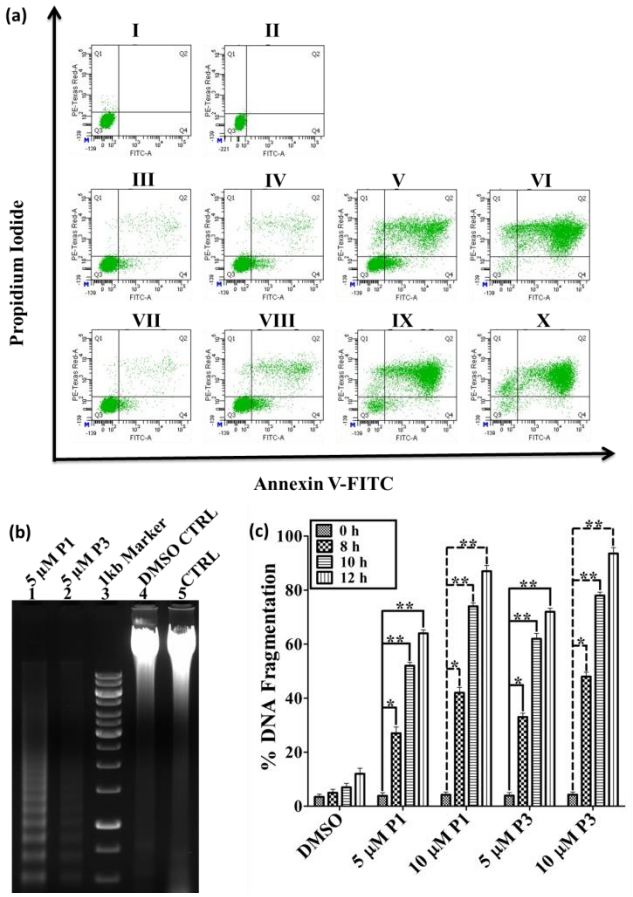

Fig. 9 (a) Flow cytometric analysis of *L. donovani* promastigote death through PCD/necrotic process using annexin V-FITC and PI in FL-1 versus FL-2 channels. Parasites were stained with FITC-annexinV and PI without any pretreatment (panel I), after 0.2% DMSO (panel II) or after amphiphilic gelator **P1** 0.5, 1.0, 2.5 and 5.0 µM (panel III to VI) and after amphiphilic gelator P3 0.5, 1.0, 2.5 and 5.0 µM (panel VII to X) for 12 h. The cells in the bottom right quadrant in each of the panels showed apoptosis, whereas cells in the top right quadrant represent late-apoptotic populations. (b) Genomic DNAs were isolated from *L. donovani* promastigotes without any treatment served as control (lane 5) after treatment with 0.2% DMSO (lane 4), 5 µM **P1** (lane 1), 5 µM **P3** (lane 2) and electrophoresed in 1.5% agarose gel. (c) Extent of genomic DNA fragmentation upon **P1** and **P3** treatment in dose-and time-dependent manner. Parasites were treated with 5.0 and 10 µM of **P1** and **P3** for the indicated time periods (0, 8, 10, and 12 h) as negative control, parasites were also treated with 0.2% DMSO. Values were obtained from the MULTISCAN EX readings at 405 nm. The percentage fragmentation is plotted for different time periods of treatment. Data represent means ± SD. (n=3). *P<0.01, **P<0.001, ***P<0.0001 compared with zero hour treatment control, by the Student t-test.

P1 and P3 induces apoptosis like cell death in *Leishmania* cells

The mode of cell death in *Leishmania donovani* parasites treated with amphiphilic gelators **P1** and **P3** was identified using fluorescein isothiocyanate (FITC)-annexinV and Propidium iodide (PI) staining kit as described in materials and methods section. Externalization of phosphatidyl serine (stained by annexinV-FITC) and presence of impermeant cell membrane (negative staining of PI) are indication of programmed cell death (PCD). On the other hand necrotic cells being permeant to PI show positive staining of nuclei, therefore discriminating rom PCD-induced parasites. The intermediate of these two distinct phenomena are showed in late apoptotic cells. Fig. 9a shows 98-99% of control parasites both PI and annexinV negative, seen in flow-cytometry analysis. Dose-dependent progression of the populations of total apoptotic cell (including both early and late apoptotic cells) were observed in treated cells (Fig. 9a). All these data clearly indicate that these treated cells undergo apoptotic-like cell death. Next, progression of apoptotic-like events activates downstream effector molecules that degrade cellular DNA, which is characteristic of PCD. To check genomic DNA fragmentation in the amphiphilic gelators **P1** and **P3** treated parasites a DNA fragmentation assay was performed. Genomic DNA was isolated from amphiphilic gelators **P1** and **P3** or 0.2% DMSO treated promastigotes after 12 h and electrophoresed in 1.5% agarose gel. Amphiphilic gelators treated parasites showed a laddering pattern which is indicative of DNA fragmentation whereas DMSO-treated parasites exhibit a single genomic DNA band in the gel. Camptothecin was used as a positive control (Fig. 9b). The extent of DNA fragmentation in amphiphilic gelators treated parasites was estimated using an ELISA-based kit (Roche Biochemicals). A dose- dependent increase in DNA fragmentation was observed in amphiphilic gelators treated cells (Fig. 9c). Amphiphilic gelators (5.0 and 10 µM) induce a considerable amount of DNA fragmentation which increased with time for the same treatment dose, while DMSO treatment failed to fragment DNA. After 10 h of treatment, 70 to 80% fragmentation of total nuclear DNA was observed and about 90 to 95% fragmentation was observed at 12 h following treatment with amphiphilic gelators (Fig. 9c). All this data indicates that the triggering of apoptosis ultimately activates different nucleases to degrade nucleosome architecture.

AFM imaging analysis

The AFM imaging analysis shows the ultrastructure disruption of *Leishmania* promastigotes architecture. This imaging analysis revealed the topographical differences in cell shape, size etc. between normal untreated and treated leishmanial cells. So far we observed that these amphiphilic gelators could induce the progression of PCD, these processes being detrimental to cells. AG83 promastigotes treated with **P1** and **P3** at 1.0, 2.5 and 5.0 µM concentration for 12 h showed altered cell architecture. Untreated or control parasites possessed typical slender cell bodies with smooth cell surface and presence of an elongated flagellum confirmed the normal design of the cell (Fig. 10a). Treated promastigotes shows shrunken morphology which is a sign of possible loss of cell volume (Fig. 10c, f) when treated with 1.0 µM of **P1** and **P3**. At a 2.5 µM concentration of amphiphilic gelators, the outer membrane got ruptured showing a typical phenotype of such

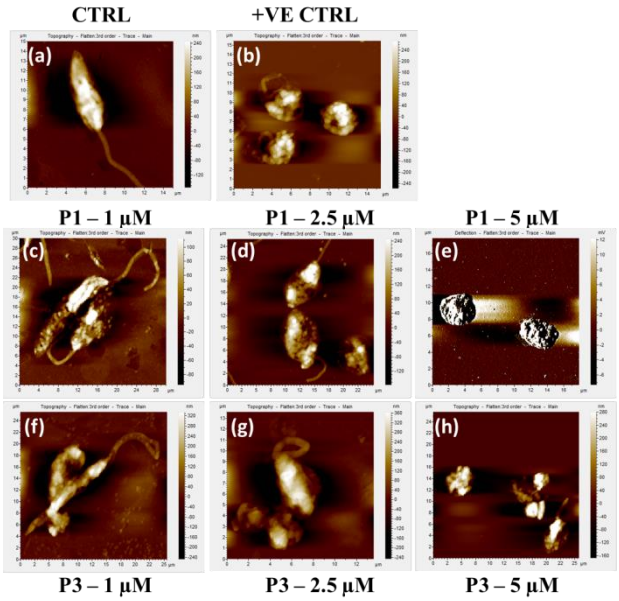

Fig. 10 (a) Atomic force microscopy (AFM) micrography of the intact promastigote. (b) Promastigotes treated with10 µM CPT. (c-e) Promastigotes treated with 1.0, 2.5 and 5.0 µM of **P1** and (f-h) Promastigotes treated with 1.0, 2.5 and 5.0 µM of **P3**.

a cell morphology (Fig. 10d, g). After increasing the concentration upto 5.0 µM for 12 h treatment complete disruption of cell morphology was observed and also they were devoid of any flagella (Fig. 10e, h).

P1 and P3 show cytotoxicity towards *Leishmania donovani* axenic amastigotes: Since, amastigotes form of *Leishmania* species are responsible for all clinical manifestations in humans and since study with intracellular amastigotes is more challenging, so the amphiphilic **P1** and **P3** were first tested against axenic amastigotes. This experiment allowed us to select the best candidates for subsequent assays with intracellular amastigotes. *Leishmania donovani* axenic amastigotes were different from promastigotes in terms of pH, temperature and culture medium. Cytotoxic potential of **P1** and **P3** against axenic amastigotes were tested using MTT assay after 12 h treatment with different concentrations of the amphiphilic gelators (Fig. 11). Interestingly, we found that IC_{50}values were more or less similar to those for infected macrophage cells. The IC_{50}values for **P1** and **P3** were found to be 0.682 µM and 0.611 µM respectively. Almost 98-99% of the total amastigotes were killed by **P1** or **P3** at 5.0 µM concentration. We conclude that these amphiphilic gelators are able to kill the deadliest intracellular form of *Leishmania donovani* amastigotes.

Table 4. EC_{50} and EC_{90} values for **P1** and **P3** on *Leishmania* amastigotes in macrophages.

Amastigotes	P1		P3		Miltefosine EC_{50} (µM)
	EC_{50} (µM)	EC_{90} (µM)	EC_{50} (µM)	EC_{90} (µM)	
AG83	0.662 ± 0.0011	1.786 ± 0.0014	0.597 ± 0.0011	1.541 ± 0.0014	11.418 ± 0.0016
Ld Major	0.682 ± 0.0012	1.553 ± 0.0016	0.611 ± 0.0013	1.451 ± 0.0016	11.812 ± 0.0012
BHU-575	0.792 ± 0.0013	1.815 ± 0.0014	0.768 ± 0.0012	1.802 ± 0.0014	12.523 ± 0.0012
MIL^R	0.891 ± 0.0012	1.914 ± 0.0013	0.877 ± 0.0011	1.873 ± 0.0013	>60
CPT^R	0.608 ± 0.0013	1.591 ± 0.0016	0.572 ± 0.0011	1.606 ± 0.0016	11.213 ± 0.0013

P1 and P3 reduce wild type and other resistant intracellular amastigotes of Leishmanial strains from murine peritoneal macrophage cells:

Finally, we also studied the effect of these amphiphilic gelators on murine peritoneal macrophages. Since it is observed thatthese amphiphilic gelators are effective against a large array of *Leishmania*strains, their cytotoxic activity on the more deadly amastigote form which is found intracellularly was examined. Primary macrophage cells were infected with early log phase promastigotes of *L. donovani* wild type AG83 strain, *L. major*, multidrug resistant BHU-575 strain, MIL^R strain and camptothecin resistant strain *in vitro*. After adherence, these macrophage cells were infected with different concentrations of both **P1** and **P3** (0.25 µM, 0.50 µM, 1.00 µM, 2.50 µM and 5.00 µM) for 12 h and intracellular amastigotes were counted. Interestingly we observed that the parasitic burden in wild type AG83 strain, *L. major*, multidrug resistant BHU-575 strain, MIL^R strain and camptothecin resistant strain was reduced to 98%, 90%, 96% 97% and 98% respectively using the highest dose of the amphiphilic gelators (5.0 µM) (Fig. 12). The EC_{50} and EC_{90} values of these amphiphilic gelators against intracellular amastigotes were measured using the variable-slope model to determine the EC_{50}, and given in table 4. Miltefosine was used as a positive control. The effects of these amphiphilic gelators on cultured murine peritoneal macrophages (Fig. 12) and mammalian normal fibroblast (L929) cells (Fig. S11) were determined using MTT assay. Results showed that treatment with 100 µM of amphiphilic gelators **P1** and **P3** killed only 10-30% of total macrophages (Fig. 12). Results showed that **P1** and **P3** amphiphiles were not cytotoxic to normal fibroblast cells. Fig. S11 shows that up to 100 µM concentration of amphiphiles more than 94% of the cells were viable. These results pointed to a right strategy in the use of these amphiphiles as anti-leishmanial agent against Wild type as well as drug resistant strains of *L. donovani*.

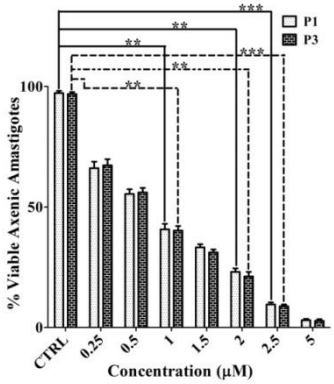

Fig. 11 Cytotoxic effect of amphiphilic gelator **P1** and **P3** on the growth of *Leishmania donovani* axenic amastigotes. Analysis of *in vitro* dose-dependent cytotoxicity of **P1** and **P3** by MTT assay. Axenic amastigotes were treated with **P1** and **P3** 0.25 µM, 0.50 µM, 1.00 µM, 1.50 µM, 2.00 µM, 2.50 µM and 5.00 µM of **P1** and **P3** for 12 h. Percentage of viable amastigotes were measured by MTT assay.

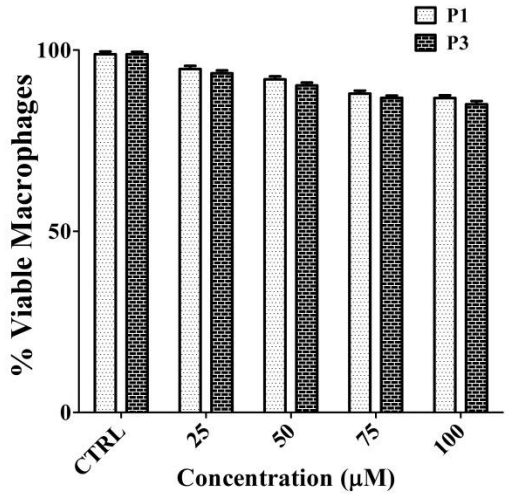

Fig. 12 Toxic effect of natural amino acid based amphiphilic gelator **P1** and **P3** on RAW 264.7 macrophages treated for 24 h with increasing concentrations of **P1** and **P3** and cell viability was assessed.

Discussion

Due to the emergence of drug resistant parasites there is a need to develop new drugs to diagnose this deadly disease. Moreover, due to unavailability of effective vaccines and chemotherapy, treatment of leishmaniasis is unsatisfactory. Thus, there is a crucial need to develop new drugs and newer therapeutic strategies.

The main rationale to synthesize gelator amphiphiles and to initiate the study was the fact that they have antibacterial property. Self-assembling amphiphilic molecules are an intriguing platform for the development of functional biomolecular actives against pathogens due to their ability to disrupt bacterial membranes and function as drug carriers. In an earlier study it was reported that an oxindoles a heterocyclic organic compound which have tryptophan like structure have great potential to kill *Leishmania*.[60] Oxindoles constitute a large array of natural products and other compounds that have great pharmaceutical value.[62-64] Oxindoles have a broad spectrum of biological activity and has been reported to have antitumour, antibacterial, insecticidal and also used for treatment of hyponatremia.[60,65,66] Based on these relevant data wed synthesize L-phenylalanine and L-tryptophan based gelator amphiphiles with variable chain length of $-NH_2$ containing cationic head groups. There are reports that L-tryptophan-containing peptides can be used as a class of antibacterial peptides.[12,58] But, in this report, thus the lack of L-tryptophan's antibacterial activity makes the results very noticeable.

In the present study, we have investigated the effect of these gelator amphiphiles on *Leishmania donovani* AG83 promastigotes *invitro*. To the best of our knowledge, this study provides the first evidence that amino acid containing amphiphiles can exhibitanti-leishmanial activity. Moreover these molecules were effective against different drug-resistant strains of *L. donovani*. Our report showed that amphiphilic **P1** and **P3** effectively kill both wild type as well as drug resistance parasites in both time and concentration dependent manner. Introduction of these amphiphilic gelators causes an increase in intracellular as well as mitochondrial ROS production. However, following pretreatment with NAC there is inhibition in the formation of ROS. The study indicates that amphiphilic gelators **P1** and **P3** are effective inducers of apoptosis in *Leishmania donovani* cells, and this is confirmed by externalization of phosphatidyl serine. Moreover, gDNA fragmentation is observed which is a hallmark of apoptosis. These data together indicate the initiation of apoptosis-like cell death in response to treatment with amphiphilic gelators. The parasite ultra-structure studies by atomic force microscope analysis also led to some interesting observations. We observed disruption of cell architecture, shortening of flagella as well as atypical cell phenotype. This investigation also provides a meticulous insight into the parasite ultra-structure alteration caused by these gelator amphiphiles. To our knowledge, this report is the first of this kind. The apoptotic pathway that initiates inside the parasite after exposure to these amphiphilic gelators was revealed, and we have shown that these compounds have promise as chemotherapeutic tools against several forms of human leishmaniasis. Microscopic studies shed light on the events occurring at the cellular level. Interestingly, the effect was more or less similar in all the strains (wild type as well as drug resistance) of trypanosomatid parasites tested here.

To confirm the accessibility of these gelator amphiphiles as a drug candidate, their effect upon human macrophage cells were evaluated. The amphiphilic gelators showed minimal cytotoxic effect on uninfected cultured murine peritoneal macrophages up to 200 μM concentration. The IC_{50} value for uninfected cultured murine peritoneal macrophages was also very high as compared to amastigotes as well as promastigotes. Further in vitro studies were performed with infected murine peritoneal macrophage cells. Interestingly the parasitic burden gradually decreased after treatment with these amphiphilic gelators up to 5.0 μM concentration.

Thus, for the first time, we have shown that amino acid-based gelator amphiphiles are effective against a large array of trypanosomatid parasites. In the current time when parasites are emerging resistance to available classical drugs, the very fact that these compounds work with equal potency against with wild type *Leishmania donovani* AG83 strain, multidrug resistant BHU-575 strain, CPT^R strain as well as MIL^R strain of the parasite and finds a way towards development of new pharmaceutical approach against this deadly disease in near future. The amphiphilic gelators **P1** and **P3** serve as lead candidate compounds for anti-leishmanial chemotherapy to combat this dreadful disease.

Conclusions

This study demonstrates the formation of hydrogels based on β-sheet fibril networks from a series of amino acid-containing amphiphilic molecules. Interestingly, two of these gels show antibacterial activity against both Gram-positive bacteria (*B. subtilis*) and Gram-negative bacteria (*P. aeruginosa* and *E. coli*). Moreover, the two gelators containing L-phenylalanine exhibit

an antiparasitic activity against several strains of *L. donovani*, including a drug-resistant strain. Interestingly, it is evident from the results that ROS generation inside the parasite and mitochondrial membrane depolarisation are the main cause of antiparasitic activity. Additionally, these gelator-based amphiphiles are minimally toxic to host macrophage cells, indicating the potential application of these gels as a therapeutic agent for leishmaniasis in the near future. The gels were comprehensively characterized by using various techniques such as thermal stability, rheology, HR-TEM, FTIR, wide-angle X-ray diffraction, and small-SAXS.

Unexpectedly, the tryptophan-containing amphiphiles show neither antibacterial nor antiparasitic activity against any type of leishmaniasis. However remarkable activity was observed for L-phenylalanine-based amphiphiles in terms of both antibacterial activity and antiparasitic activity against leishmaniasis.

Author Contributions

The manuscript was written through contributions of all authors. All authors have given approval to the final version of the manuscript.

Conflicts of interest

There are no conflicts to declare.

Acknowledgements

B. M. would like to acknowledge UGC, New Delhi, India and IACS; V. K. G. would like to acknowledge ICMR, New Delhi India for the award of ICMR-JRF fellowship. B. H. would like to acknowledge UGC and IACS; T. M. would like to acknowledge CSIR, New Delhi, India for their financial support. We thank Dr. Arun Bandyopadhyay, Director, CSIR-IICB, Kolkata for his interest in this work. We are thankful to Dr. Syamal Roy, CSIR-IICB, Kolkata for the kind gift of the drug resistant parasites. We are also thankful to Mr. T. Muruganandan for helping in AFM studies and Mr. Tanmoy Dalui for helping in Flow-cytometric analysis. C.J.C. E-G. thanks Diamond Light Source and the University of Reading for sponsorship of her postgraduate study, and we thank Diamond Light Source for the award of beamtime, reference SM21470-3.

Notes and references

1 M. Tena-Solsona, D. Marson, A. C. Rodrigo, S. M. Bromfield, B. Escuder, J. F. Miravet, N. Apostolova, E. Laurini, S. Pricl and D. K. Smith, *Biomater. Sci.*, 2019, **7**, 3812–3820.

2 A. Pettignano, S. Grijalvo, M. Häring, R. Eritja, N. Tanchoux, F. Quignard and D. Díaz Díaz, *Chem. Commun.*, 2017, **53**, 3350–3353.

3 W. Ji, Y. Tang, P. Makam, Y. Yao, R. Jiao, K. Cai, G. Wei and E. Gazit, *J. Am. Chem. Soc.*, 2021, **143**, 17633–17645.

4 M. Samateh, S. S. Sagiri, R. Sanni, C. A. Chee, S. Satapathy and G. John, *J. Agric. Food Chem.*, 2020, **68**, 13282–13290.

5 A. S. Pina, L. Morgado, K. L. Duncan, S. Carvalho, H. F. Carvalho, A. J. M. Barbosa, B. de P. Mariz, I. P. Moreira, D. Kalafatovic, B. M. Morais Faustino, V. Narang, T. Wang, C. G. Pappas, I. Ferreira, A. C. A. Roque and R. V. Ulijn, *Chem. Sci.*, 2022, **13**, 210–217.

6 G. Grover and R. G. Weiss, *Gels*, 2021, **7**, 19.

7 S. Panja, B. Dietrich and D. J. Adams, *Angew. Chemie - Int. Ed.*, 2022, **61**, 1–6.

8 N. Singh, M. Kumar, J. F. Miravet, R. V. Ulijn and B. Escuder, *Chem. - A Eur. J.*, 2017, **23**, 981–993.

9 D. B. Amabilino, D. K. Smith and J. W. Steed, *Chem. Soc. Rev.*, 2017, **46**, 2404–2420.

10 W. Liyanage, K. Vats, A. Rajbhandary, D. S. W. Benoit and B. L. Nilsson, *Chem. Commun.*, 2015, **51**, 11260–11263.

11 V. Castelletto and I. W. Hamley, *ACS Nano*, 2022, **16**, 1857–1867.

12 J. Zhang, S. Liu, H. Li, X. Tian and X. Li, *Langmuir*, 2020, **36**, 11316–11323.

13 A. D'Souza, J. H. Yoon, H. Beaman, P. Gosavi, Z. Lengyel-Zhand, A. Sternisha, G. Centola, L. R. Marshall, M. D. Wehrman, K. M. Schultz, M. B. Monroe and O. V. Makhlynets, *ACS Appl. Mater. Interfaces*, 2020, **12**, 17091–17099.

14 S. Basak, N. Nandi, S. Paul, I. W. Hamley and A. Banerjee, *Chem. Commun.*, 2017, **53**, 5910–5913.

15 S. S. Lee, E. L. Hsu, M. Mendoza, J. Ghodasra, M. S. Nickoli, A. Ashtekar, M. Polavarapu, J. Babu, R. M. Riaz, J. D. Nicolas, D. Nelson, S. Z. Hashmi, S. R. Kaltz, J. S. Earhart, B. R. Merk, J. S. McKee, S. F. Bairstow, R. N. Shah, W. K. Hsu and S. I. Stupp, *Adv. Healthcare Mater.,* 2015, **4**, 131−141.

16 D. Bairagi, P. Biswas, K. Basu, S. Hazra, D. Hermida-Merino, D. K. Sinha, I. W. Hamley and A. Banerjee, *ACS Appl. Bio Mater.*, 2019, **2**, 5235–5244.

17 C. Ligorio, A. Vijayaraghavan, J. A. Hoyland and A. Saiani, *Acta Biomater.*, 2022, **143**, 145–158.

18 K. Basu, A. Baral, S. Basak, A. Dehsorkhi, J. Nanda, D. Bhunia, S. Ghosh, V. Castelletto, I. W. Hamley and A. Banerjee, *Chem. Commun.*, 2016, **52**, 5045–5048.

19 L. Qin, F. Xie, P. Duan and M. Liu, *Chem. - A Eur. J.*, 2014, **20**, 15419–15425.

20 R. Martí-Centelles, I. Dolz-Pérez, J. De la O, I. Ontoria-Oviedo, P. Sepúlveda, V. J. Nebot, M. J. Vicent and B. Escuder, *ACS Appl. Bio Mater.*, 2021, **4**, 935–944.

21 I. W. Hamley, *ACS Appl. Bio Mater.*, 2022, **5**, 905–944.

22 K. Basu, N. Nandi, B. Mondal, A. Dehsorkhi, I. W. Hamley and A. Banerjee, *Interface Focus*, 2017, **7**, 20160128.

23 B. Mondal, D. Bairagi, N. Nandi, B. Hansda, K. S. Das, C. J. C. Edwards-Gayle, V. Castelletto, I. W. Hamley and A. Banerjee, *Langmuir*, 2020, **36**, 12942–12953.

24 Z. Yang, G. Liang, M. Ma, A. S. Abbah, W. W. Lu and B. Xu, *Chem. Commun.*, 2007, 843–845.

25 A. Baral, S. Roy, S. Ghosh, D. Hermida-Merino, I. W. Hamley and A. Banerjee, *Langmuir*, 2016, **32**, 1836–1845.

26 E. R. Cross, S. M. Coulter, A. M. Fuentes-Caparrós, K. McAulay, R. Schweins, G. Laverty and D. J. Adams, *Chem. Commun.*, 2020, **56**, 8135–8138.

27 N. Nandi, K. Gayen, S. Ghosh, D. Bhunia, S. Kirkham, S. K. Sen, S. Ghosh, I. W. Hamley and A. Banerjee, *Biomacromolecules*, 2017, **18**, 3621–3629.

28 A. S. Veiga and J. P. Schneider, *Biopolymers*, 2013, **100**, 637–644.

29 E. Ji, A. Parthasarathy, T. S. Corbitt, K. S. Schanze and D. G. Whitten, *Langmuir*, 2011, **27**, 10763–10769.

30 E. Pazos, E. Sleep, C. M. R. Pérez, S. S. Lee, F. Tantakitti and S. I. Stupp, *J. Am. Chem. Soc.*, 2016, **138**, 5507–5510.

31 V. Castelletto, C. J. C. Edwards-Gayle, I. W. Hamley, G. Barrett, J. Seitsonen and J. Ruokolainen, *ACS Appl. Mater. Interfaces,* 2019, **11**, 9893-9903.
32 N. Mukherjee, A. Adak and S. Ghosh, *Soft Matter*, 2020, **16**, 10046−10064.
33 S. Basak, J. Nanda, A. Banerjee, *J. Mater. Chem.* 2012, **22**, 11658-11664.
34 A. Adak, S. Ghosh, V. Gupta and S. Ghosh, *Biomacromolecules*, 2019, **20**, 1889−1898.
35 D. S. S. M. Uppu, S. Samaddar, J. Hoque, M. M. Konai, P. Krishnamoorthy, B. R. Shome and J. Haldar, *Biomacromolecules*, 2016, **17**, 3094–3102.
36 C. J. C. Edwards-Gayle, V. Castelletto, I. W. Hamley, G. Barrett, F. Greco, D. Hermida-Merino, R. Rambo, J. Seitsonen and J. Ruokolainen, *ACS Appl. Bio Mater.* 2019, **2**, 2208-2218.
37 C. J. C. Edwards-Gayle, G. Barrett, S. Roy, V. Castelletto, J. Seitsonen, J. Ruokolainen and I. W. Hamley, *ACS Appl. Bio Mater.* 2020, **3**, 1165-1175.
38 S. Fernandez-Lopez, H. S. Kim, E. C. Choi, M. Delgado, J. R. Granja, A. Khasanov, K. Kraehenbuehl, G. Long, D. A. Weinberger, K. M. Wilcoxen and M. R. Ghadiri, *Nature*, 2001, **412**, 452–455.
39 H. Hashizume, R. Sawa, K. Yamashita, Y. Nishimura and M. Igarashi, *J. Antibiot.*, 2017, **70**, 699–704.
40 O. Bellotto, S. Kralj, M. Melchionna, P. Pengo, M. Kisovec, M. Podobnik, R. De Zorzi and S. Marchesan, *ChemBioChem*, 2022, **23**, e202100518.
41 P. Sriwongpan, S. Nedsuwan, J. Manomat, S. Charoensakulchai, K. Lacharojana, J. Sankwan, N. Kobpungton, T. Sriwongpun, S. Leelayoova, M. Mungthin, S. Siripattanapipong, T. Ruang-Areerate, T. Naaglor, T. Eamchotchawalit and P. Piyaraj, *PLoS Negl. Trop. Dis.*, 2021, **15**, e0009545.
42 F. Chappuis, S. Sundar, A. Hailu, H. Ghalib, S. Rijal, R. W. Peeling, J. Alvar and M. Boelaert, *Nat. Rev. Microbiol.*, 2007, **5**, 873–882.
43 E. Torres-Guerrero, M. R. Quintanilla-Cedillo, J. Ruiz-Esmenjaud and R. Arenas, *F1000Research*, 2017, **6**, 750.
44 M. A. Cunha, B. J. Celeste, N. Kesper, M. Fugimori, M. M. Lago, A. S. Ibanes, L. M. Ouki, E. A. S. Neto, F. F. Fonseca, M. A. L. Silva, W. L. B. Júnior and J. A. L. Lindoso, *BMC Infect. Dis.*, 2020, **20**, 885.
45 S. Sundar and J. Jaya, *J. Glob. Infect. Dis.*, 2010, **2**, 159–166.
46 T. R. N. Berbert, T. F. P. De Mello, P. Wolf Nassif, C. A. Mota, A. V. Silveira, G. C. Duarte, I. G. Demarchi, S. M. A. Aristides, M. V. C. Lonardoni, J. J. Vieira Teixeira and T. G. V. Silveira, *Dermatol. Res. Pract.*, 2018, **2018**, 1–21.
47 J. Chakravarty and S. Sundar, *J. Glob. Infect. Dis.*, 2010, **2**, 167–176.
48 N. Shakya, P. Bajpai and S. Gupta, *J. Parasit. Dis.*, 2011, **35**, 104–112.
49 V. Castelletto, C. J. C. Edwards-Gayle, F. Greco, I. W. Hamley, J. Seitsonen and J. Ruokolainen, *ACS Appl. Mater. Interfaces* 2019, **11**, 33573-33580.
50 K. K. Banoth, Faheem, K. V. G. ChandraSekhar, N. Adinarayana and S. Murugesan, *Heliyon*, 2020, **6**, e04916.
51 R. Basu, S. Bhaumik, J. M. Basu, K. Naskar, T. De and S. Roy, *J. Immunol.*, 2005, **174**, 7160–7171.
52 S. Chowdhury, T. Mukherjee, S. R. Chowdhury, S. Sengupta, S. Mukhopadhyay, P. Jaisankar and H. K. Majumder, *Antimicrob. Agents Chemother.*, 2014, **58**, 2186–2201.
53 A. Roy, B. B. Das, A. Ganguly, S. Bose Dasgupta, N. V. M. Khalkho, C. Pal, S. Dey, V. S. Giri, P. Jaisankar, S. Dey and H. K. Majumder, *Biochem. J.*, 2008, **409**, 611–622.
54 A. Ghosh, S. Bhattacharjee, S. P. Chowdhuri, A. Mallick, I. Rehman, S. Basu and B. B. Das, *Sci. Adv.*, 2019, **5**, eaax9778.
55 C. Batandier, E. Fontaine, C. Kériel and X. M. Leverve, *J. Cell. Mol. Med.*, 2002, **6**, 175–187.
56 A. Boveris and B. Chance, *Biochem. J.*, 1973, **134**, 707–716.
57 A. Boveris, N. Oshino and B. Chance, *Biochem. J.*, 1972, **128**, 617–630.
58 D. I. Chan, E. J. Prenner and H. J. Vogel, *Biochim. Biophys. Acta – Biomembranes,* 2006, **1758**, 1184-1202.
59 N. Sen, B. B. Das, A. Ganguly, T. Mukherjee, G. Tripathi, S. Bandyopadhyay, S. Rakshit, T. Sen and H. K. Majumder, *Cell Death Differ.* **2004**, *11*, 924–936.
60 M. Mattiazzi, C. Vijayvergiya, C. D. Gajewski, D. C. DeVivo, G. Lenaz, M. Wiedmann and G. Manfredi, *Hum. Mol. Genet.*, 2004, **13**, 869–879.
61 S. Dingley, K. A. Chapman and M. J. Falk, *Methods Mol. Biol.*, 2012, **837**, 231–239.
62 S. Saha, C. Acharya, U. Pal, S. R. Chowdhury, K. Sarkar, N. C. Maiti, P. Jaisankar and H. K. Majumder, *Antimicrob. Agents Chemother.*, 2016, **60**, 6281–6293.
63 J. Li, N. Wang, C. Li and X. Jia, *Chem. - A Eur. J.*, 2012, **18**, 9645–9650.
64 N. Lashgari and G. M. Ziarani, *Arkivoc*, 2012, **1**, 277–320.
65 H. Venkatesan, M. C. Davis, Y. Altas, J. P. Snyder and D. C. Liotta, *J. Org. Chem.*, 2001, **66**, 3653–3661.
66 Â. Monteiro, L. M. Gonçalves and M. M. M. Santos, *Eur. J. Med. Chem.,* 2014, **79**, 266–272.